

The Inert Doublet Model and its extensions*

MARIA KRAWCZYK, NEDA DARVISHI, DOROTA SOKOŁOWSKA

Faculty of Physics, University of Warsaw
ul. Pasteura 5, 02-093 Warsaw, Poland

The Inert Doublet Model and its extension with an additional complex singlet is considered. The CP violation aspects are analysed in the simplified case, with one SM-like Higgs doublet and a complex singlet.

PACS numbers: 12.60.Fr, 14.80.Ec, 14.80.Fd, 95.35.+d

1. Introduction

A 125 GeV Higgs-like particle discovered at the LHC in 2012 has properties expected in the Standard Model (SM). However, as it is well known, the SM-like Higgs scenario appears in various models, among them in models with two Higgs doublets (2HDM). Models with more doublets, as well as with singlets, can be also considered, all leading to $\rho = \frac{M_W^2}{M_Z^2 \cos^2 \theta_W} = 1$ at the tree-level, very close to the observed value.

The SM-like Higgs scenario, as well as a stable scalar Dark Matter (DM), appears naturally within the Inert Doublet Model (IDM) – a version of the Two Higgs Doublet Model with an exact discrete $D(Z_2)$ symmetry [1, 2, 3]. This model is in agreement with current data, both from accelerator and astrophysical experiments [4, 5]. It has been applied to describe the temperature evolution of the Universe in T^2 -approximation [6]. There are possible sequences of phase transitions in the early Universe, that may lead to the current phase with a DM candidate in one, two or three steps. Using an effective potential approach with one-loop $T = 0$ Weinberg-Coleman term and temperature-dependent effective potential at $T \neq 0$ it was found, that the strong first-order phase transition needed for baryogenesis can be realized in the IDM; moreover, a region with a good DM relic density and a strong first-order phase transition exists [7]. However, the IDM cannot be a correct model for baryogenesis, because the CP violation occurs in this

* Presented at Zakopane School 2015 by M. Krawczyk and N. Darvishi.

model as in the SM, i.e. only in the CKM matrix, which is well-known to be not sufficient. Therefore, an extension of the IDM is desired.

One of the option is adding one extra complex singlet of the scalar fields. We have studied this model, called the IDMS, in Ref. [8]. We chose to have spontaneous CP violation in the model through a non-zero complex vacuum expectation value (VEV) of the singlet. There are three Higgs particles with no definite CP properties; the lightest one among them can play a role of a SM-like 125 GeV Higgs particle. On the other hand, the lightest neutral scalar from the inert sector remains a viable DM candidate. Due to the extended Higgs sector, new interesting phenomena appear in the study of relic density, including new annihilation channels, interference between various Higgs contributions, and heavy Higgs resonance annihilation.

Detailed analysis of CP properties of the IDMS is rather complicated, so we have decided to consider first these properties in the simplified model, consisting of the SU(2) doublet and a complex singlet with non-zero VEV, which is a part of our IDMS framework. We found that to have the CP violation one non-zero cubic term in the singlet potential is needed.

In this work we present the IDM (section 2), together with its extension, the IDMS (section 3). We also discuss in details the differences between two models. The simplified case, with one SM-like Higgs doublet and a complex singlet (SM+CS), is presented in section 4.

2. The IDM

Here we consider a particular version of 2HDM – the Inert Doublet Model (IDM), which is very similar to the SM, as only one SU(2) doublet, Φ_S , is involved in the Spontaneous Symmetry Breaking (SSB), and there exists only one SM-like Higgs particle. The properties of the second doublet, Φ_D , are quite different: it is not involved in the SSB and does not interact with fermions. It contains four dark (inert) scalars, which have limited interactions with the SM particles and the lightest of them is stable, thus, if neutral, being a good candidate for Dark Matter.

The real content of the theory is determined by the symmetry properties of the Lagrangian, as well as of the vacuum state. We assume that the potential and the Yukawa interaction (only Φ_S interacts with fermions) are Z_2 -symmetric with respect to the transformation $\Phi_S \rightarrow \Phi_S$, $\Phi_D \rightarrow -\Phi_D$, which we call the D symmetry. Note, that this symmetry leads to the CP conservation in the model. The D -symmetric potential has the following form:

$$V = -\frac{1}{2} \left[m_{11}^2 (\Phi_S^\dagger \Phi_S) + m_{22}^2 (\Phi_D^\dagger \Phi_D) \right] + \frac{\lambda_1}{2} (\Phi_S^\dagger \Phi_S)^2 + \frac{\lambda_2}{2} (\Phi_D^\dagger \Phi_D)^2 \\ + \lambda_3 (\Phi_S^\dagger \Phi_S) (\Phi_D^\dagger \Phi_D) + \lambda_4 (\Phi_S^\dagger \Phi_D) (\Phi_D^\dagger \Phi_S) + \frac{\lambda_5}{2} \left[(\Phi_S^\dagger \Phi_D)^2 + (\Phi_D^\dagger \Phi_S)^2 \right],$$

with all parameters real. We take $\lambda_5 < 0$ without loss of generality [6].

Various extrema can be realized in this potential. The possible vacuum expectation values (VEVs) are as follows:

$$\langle \Phi_S \rangle = \begin{pmatrix} 0 \\ \frac{1}{\sqrt{2}} v_S \end{pmatrix}, \quad \langle \Phi_D \rangle = \begin{pmatrix} u \\ \frac{1}{\sqrt{2}} v_D \end{pmatrix} \quad v_S, v_D, u \in R. \quad (1)$$

Neutral extrema are realized for $u = 0$. There are four types of neutral extrema (and also vacua) that have different symmetry properties:

- (i) The EWs case with $u = v_D = v_S = 0$ corresponds to the electroweak (EW) symmetry.
- (ii) Mixed vacuum (M) with $u = 0, v_S \neq 0, v_D \neq 0$. There exist charged Higgs particles H^\pm , a pseudoscalar Higgs A and two CP-even Higgses h and H , either of them could be SM-like.
- (iii) Inert vacuum (I_1) with $u = v_D = 0, v_S \neq 0, v_S^2 = m_{11}^2/\lambda_1$, conserves the D -parity and assures the existence of a stable scalar particle.
- (iv) Inertlike vacuum (I_2) with $u = v_S = 0, v_D \neq 0$. This vacuum spontaneously violates the D symmetry by $v_D \neq 0, v_D^2 = m_{22}^2/\lambda_2$. Fermions are massless.

If $u \neq 0$ then the charged vacuum (CB) is realized, with the $U(1)_{\text{QED}}$ symmetry breaking and the appearance of a massive photon. Such a case is not realized in the nature today. Mixed and charged minima cannot exist for the same values of the parameters of the potential V . On the other hand, minima of the inert-type (I_1 or I_2) can overlap one another and with M and CB minima in the (λ_4, λ_5) parameter plane [9].

A stable vacuum (i.e. extremum with the lowest energy) exists only if positivity conditions hold

$$\lambda_1 > 0, \quad \lambda_2 > 0, \quad \lambda_3 + \sqrt{\lambda_1 \lambda_2} > 0, \quad \lambda_{345} + \sqrt{\lambda_1 \lambda_2} > 0, \quad (2)$$

($\lambda_{345} = \lambda_3 + \lambda_4 + \lambda_5$) so that

$$R = \frac{\lambda_{345}}{\sqrt{\lambda_1} \sqrt{\lambda_2}} > -1.$$

VEVs (1) are related to the parameters of the potential through the extremum conditions, and so the various values of v_S, v_D, u can be represented on the phase diagram (μ_1, μ_2) , where $\mu_1 = \frac{m_{11}^2}{\sqrt{\lambda_1}}$, $\mu_2 = \frac{m_{22}^2}{\sqrt{\lambda_2}}$. Different regions of this parameter space correspond to the different vacua. There are

three regimes of parameter R , $R > 1$, $0 < R < 1$, $-1 < R < 0$, which correspond to very different phase patterns. Note, that only for $R > 1$ there is a unique possibility of coexistence of two inert-type minima, I_1 and I_2 [10, 11, 12].

In the Inert Doublet Model I_1 is the vacuum state. Here only one doublet (Φ_S) is involved in the SSB and there is only one SM-like Higgs boson h – we assume that its mass is equal to 125 GeV. The doublet Φ_D is inert (it has $\text{VEV} = 0$) and contains four scalars H , A , H^\pm . Yukawa interactions are as in Model I of 2HDM, since Φ_D does not interact with fermions. The D symmetry is exact here and the lightest neutral scalar H (or A) may play a role of DM. We take $\text{DM} = H$ (so $\lambda_4 + \lambda_5 < 0$).

Masses of the scalar particles read:

$$M_h^2 = \lambda_1 v^2 = m_{11}^2,$$

$$M_{H^\pm}^2 = \frac{\lambda_3 v^2 - m_{22}^2}{2}, M_A^2 = M_{H^\pm}^2 + \frac{\lambda_4 - \lambda_5}{2} v^2, M_H^2 = M_{H^\pm}^2 + \frac{\lambda_4 + \lambda_5}{2} v^2,$$

with $v = 246$ GeV.

Parameter λ_1, m_{11}^2 are fixed by the mass of 125 GeV Higgs particle, parameter λ_{345} is related to triple and quartic couplings between the SM-like Higgs h and the DM candidate H , λ_2 gives the quartic DM self-couplings, while λ_3 describes the Higgs particle interaction with charged scalars. These parameters are subject to various theoretical and experimental constraints (see e.g. [3], [13]–[21], [9], [22]–[29]).

In particular, perturbative unitarity leads to the following limits for self-couplings [29]:

$$\lambda_{1,2}^{\max} = 8.38, \quad \lambda_3 \in (-1.32, 16.53), \quad \lambda_{345} \in (-1.45, 12.38).$$

Above conditions, combined with requirement that I_1 is a global minimum [6], lead to [29]:

$$m_{22}^2 \lesssim 9 \cdot 10^4 \text{GeV}^2.$$

Also EWPT strongly constrain physics beyond SM. Important radiative corrections to gauge bosons propagators can be parametrized by the oblique parameters S and T [30]. Values of these parameters are demanded to lie within 2σ ellipses in the (S, T) plane, with the following central values [31]: $S = 0.03 \pm 0.09$, $T = 0.07 \pm 0.08$, with correlation equal to 87%. The LEP II analysis (reinterpretation of the MSSM analysis for the IDM) excludes the region of masses where simultaneously: $M_H < 80$ GeV, $M_A < 100$ GeV and $M_A - M_H > 8$ GeV. For $M_A - M_H < 8$ GeV the LEP I limit $M_H + M_A > M_Z$ applies [22, 23]. The LEP limit for M_{H^\pm} is: $M_{H^\pm} \gtrsim 70$ GeV [24].

Note, that direct measurements of quartic self-coupling for dark scalars λ_2 is doubtful. However, there are some indirect constraints for λ_2 that

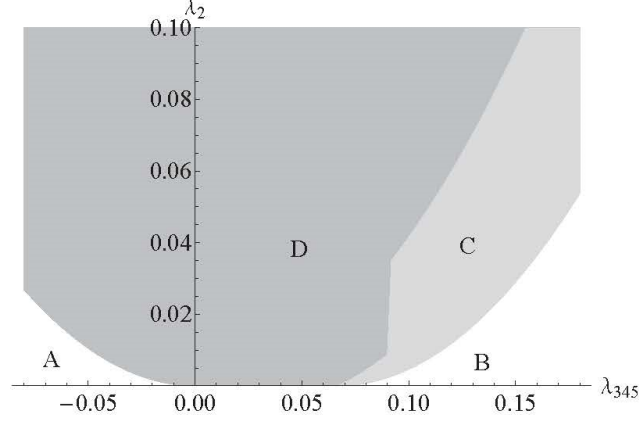


Fig. 1. Parameter space $(\lambda_{345}, \lambda_2)$ showing the coexistence of minima I_1 and I_2 . Region A is excluded by positivity constraints. I_1 and I_2 coexist in regions B and C. In region B I_2 is the global minimum, while I_1 is local, in region C the situation is reversed. In region D only minimum I_1 exists, from [32].

come from its relation to λ_{345} through the vacuum stability constraints (2) and existence of I_1 vacuum [10, 12], see Fig.(1).

2.1. LHC Higgs data constraining parameters of the IDM

The relevant LHC data on the discovered Higgs particle constraining parameters of the IDM are:

- Higgs mass $M_h = 125.09 \pm 0.24$ GeV [33],
- Higgs total decay width $\Gamma_{\text{tot}} = (4.2 - 5.5) \times 4.5$ MeV [34],
- Higgs total signal strength¹ $\mathcal{R} = 1.09 \pm 0.11$ [35],
- Higgs decay into $\gamma\gamma$ signal strength $\mathcal{R}_{\gamma\gamma} = 1.16^{+0.20}_{-0.18}$ [35],
- Invisible decay branching ratio $\text{Br}(h \rightarrow \text{inv}) < 0.23 - 0.36$ [36].

Obviously, the Higgs boson in the IDM, h , has tree-level decays to the SM particles as in the SM, however decays $h \rightarrow \text{SM SM}$, which are absent at the tree level, may differ slightly, e.g. $h \rightarrow gg, \gamma\gamma, Z\gamma$ proceeding via the loop couplings. These channels cannot change the total decay width of h considerably. Much more important in this respect are new tree-level decay

¹ Signal strength is often denoted by μ .

channels, which are absent in the SM. In the IDM there are decays of h to inert particles, among them the $h \rightarrow HH$, called the invisible decay. The recent detailed analysis shows that the IDM is in agreement with all current LHC data [5].

Other attempts undertaken at the LHC to constrain DM in processes independently from the Higgs sector, e.g. monojets or monophotons events, are not leading to important limits for the IDM. This is mainly because the IDM is a Higgs-portal DM model, where interaction between DM and SM particles are dominated by exchange of Higgs particle, with mass 125 GeV, while experimental analyses are based on effective coupling with heavy portal-particles.

2.1.1. Higgs Invisible decays

The Higgs boson of the IDM, apart from the SM decay channels, has additional ones: to a pair of dark particles, AA , HH or $H^\pm H^\mp$. The decay width for the process $h \rightarrow HH$ reads (see e.g. Ref. [4])

$$\Gamma(h \rightarrow HH) = \frac{\lambda_{345}^2 v^2}{32\pi M_h} \sqrt{1 - \frac{4M_H^2}{M_h^2}},$$

where $\lambda_{345} = \lambda_3 + \lambda_4 + \lambda_5$ is the coupling between the Higgs boson and a pair of DM particles. For the decay $h \rightarrow AA$ the parameters λ_{345} and M_H have to be replaced by $\lambda_{345}^- = \lambda_3 + \lambda_4 - \lambda_5$ and M_A , respectively.

The branching ratio of the Higgs boson decay to invisible particles is constrained by the LHC measurements, since the decay width depends on the mass of the product of the decay and its coupling to the Higgs boson. In the same way the measurement of the total Higgs decay width can be used. Below, for the sake of simplicity, we will assume that A is too heavy for the $h \rightarrow AA$ process to be allowed, i.e. only $M_H < M_h/2$. The allowed region on λ_{345} and M_H coming from the constraint on $\text{Br}(h \rightarrow \text{invisible}) < 0.37$ [36] and on the total width $\Gamma(h) < 5.4 \Gamma(h)^{\text{SM}}$ [34] corresponds to a small range around zero, $|\lambda_{345}| < 0.05$, for masses of H below 62.5 GeV.

2.1.2. Higgs decays to $\gamma\gamma$

The results of measurements of Higgs decays to $\gamma\gamma$, mentioned above, are close to the SM predictions, $\mathcal{R}_{\gamma\gamma} = 1$.

Let us define $R_{\gamma\gamma}$ (see e.g. Refs. [37, 38, 39])

$$\mathcal{R}_{\gamma\gamma} := \frac{\sigma(pp \rightarrow h \rightarrow \gamma\gamma)^{\text{IDM}}}{\sigma(pp \rightarrow h \rightarrow \gamma\gamma)^{\text{SM}}} \approx \frac{\text{Br}(h \rightarrow \gamma\gamma)^{\text{IDM}}}{\text{Br}(h \rightarrow \gamma\gamma)^{\text{SM}}}, \quad (3)$$

where the approximation of the narrow width of h and the fact that the gluon fusion dominates in the Higgs production were used, and therefore $\sigma(pp \rightarrow h)$ is the same in the IDM and the SM.

The $\text{Br}(h \rightarrow \gamma\gamma)^{\text{IDM}}$ depends both on the partial decay width of the Higgs boson to two photons, and on the total decay width of the Higgs particle. Note that, to a good approximation, only the invisible channels modify the total decay width of the Higgs boson with respect to the SM. Note that once the invisible channels are kinematically allowed, they dominate over the SM channels, so in general they tend to suppress $R_{\gamma\gamma}$.

In the SM the $h \rightarrow \gamma\gamma$ decay is induced by a W^\pm boson loop and a fermionic loops (the top quark dominates). $\Gamma(h \rightarrow \gamma\gamma)$ in the IDM differs from the one computed in the SM, because of the charged scalar, H^\pm , which gives an extra contribution to the process. This contribution can interfere either constructively or destructively with the SM part, so $\text{Br}(h \rightarrow \gamma\gamma)^{\text{IDM}}$ can be enhanced or suppressed with respect to the SM.

Let us first analyse the consequences of enhanced signal strength (we follow Ref. [39]). It was found that for $M_H < M_h/2 \approx 62.5 \text{ GeV}$ the diphoton signal strength is always suppressed with respect to the SM, due to enhancement of the total decay width of h . This means that if enhancement of the signal strength is observed, DM with mass below 62.5 GeV is excluded. Note, that if $\mathcal{R}_{\gamma\gamma} > 1.2$, then only fairly light charged scalar and H (as $M_H < M_{H^\pm}$) are allowed, with $M_{H^\pm}, M_H \lesssim 154 \text{ GeV}$.

The case where we allow $\mathcal{R}_{\gamma\gamma}$ to go below 1 will be analysed in the next section, and combined with the DM measurements.

2.2. Relic density constraints

The IDM provides a good DM candidate (H) in agreement with the data on relic density $\Omega_{DM} h^2$, $\Omega_{DM} h^2 = 0.1199 \pm 0.0027$ [40], in three regions of M_H , see eg. [3, 10], [12]–[16], [19]–[21], [25, 26]:

- light DM particles with masses below 10 GeV. Other dark particles are much heavier than DM and so this scenario mimics the behavior of the singlet DM model. As the Higgs-DM coupling needed to obtain proper relic density in this region is relatively large, this region of masses is excluded by combined results of relic density measurements and LHC data on Higgs invisible decays [4].
- medium mass regime of 50 – 150 GeV with two distinctive regions: with and without coannihilation of H with the neutral D -odd particle A . Coannihilation channels are present, if the mass difference(s) between H and other scalar particle(s) are small. For both cases, i.e. with and without coannihilation of H and A , the allowed region of λ_{345} is symmetric around zero for masses $M_H \lesssim 72 \text{ GeV}$.

Usually, very small values of λ_{345} are excluded due to a non efficient DM annihilation. If coannihilation channels are open, allowed values of λ_{345} are smaller than if coannihilation channels are closed, as the process $HH \rightarrow h \rightarrow \bar{f}f$ with the cross-section $\sigma \sim \lambda_{345}^2$ does not have to be that efficient to provide the proper relic density value. As mass increases, the region of proper relic density shifts towards the negative values of λ_{345} , which is due to opening of the annihilation channels into the gauge bosons final state and interference of processes $HH \rightarrow h \rightarrow VV$ and $HH \rightarrow VV$. For the IDM, it is possible to obtain correct relic density for masses up to 150 GeV. However, larger values of masses, which correspond to larger values of λ_{345} , are excluded by direct detection limits coming from LUX experiment.

- heavy DM of mass larger than 525 GeV. In this region all dark particles have almost degenerate masses and coannihilation processes between all dark particles are crucial for the agreement with the measured DM relic density.

The relic density data can be used to constrain λ_{345} coupling for chosen values of masses of H and other scalars [19, 13]. The same coupling, related to Higgs-charged scalar coupling λ_3 , influences the values of $\mathcal{R}_{\gamma\gamma}$ [4]. It was found that for DM with masses $M_H < M_W$ it is not possible to have an enhancement in the $h \rightarrow \gamma\gamma$ signal, and, at the same time, to be in agreement with relic density constraints. In this region $\mathcal{R}_{\gamma\gamma}$ is always below the SM value, unless the DM relic density is too small. For heavy DM candidate, as the DM influence on the Higgs sector is reduced, $\mathcal{R}_{\gamma\gamma} \approx 1$.

3. The IDMS

The IDM provides a viable DM candidate in a wide range of DM masses. However, it lacks one important ingredient needed to explain the matter-antimatter asymmetry of the Universe, namely an additional, with respect to the SM, source of CP violation. In this section we present a model which can provide this desired addition, the IDMS, i.e. the IDM plus a complex singlet [8]. The IDMS is a Z_2 -symmetric model that contains a SM-like Higgs doublet Φ_1 , as well as an inert scalar doublet Φ_2 , which has $\text{VEV}=0$ and is odd under a Z_2 symmetry, and the neutral complex singlet χ , with hypercharge $Y = 0$ and a non-zero complex VEV.²

There are different choices of symmetries in this kind of model that can lead to different phenomenology. Here, we shall assume that the symmetry

² Here we use notation Φ_1 and Φ_2 for the SM-like doublet and the inert doublet, respectively.

assignment is as follows:

$$Z_2 : \Phi_1 \rightarrow \Phi_1, \Phi_2 \rightarrow -\Phi_2, \text{ SM fields} \rightarrow \text{ SM fields}, \chi \rightarrow \chi. \quad (4)$$

This choice results in an inert sector just like in the IDM, while the Higgs sector consists of both Φ_1 and χ . In our model only Z_2 -even fields Φ_1 and χ acquire vacuum expectation values, leading to the following field decomposition around the vacuum state $(v, 0, we^{i\xi})$, where $v, w, \xi \in \mathbf{R}$:

$$\Phi_1 = \begin{pmatrix} \phi_1^+ \\ \frac{1}{\sqrt{2}}(v + \phi_1 + i\phi_6) \end{pmatrix}, \quad \Phi_2 = \begin{pmatrix} \phi_2^+ \\ \frac{1}{\sqrt{2}}(\phi_4 + i\phi_5) \end{pmatrix}, \quad (5)$$

$$\chi = \frac{1}{\sqrt{2}}(we^{i\xi} + \phi_2 + i\phi_3). \quad (6)$$

For simplicity we will consider the constrained potential, the cIDMS [8]:

$$\begin{aligned} V = & -\frac{1}{2} \left[m_{11}^2 \Phi_1^\dagger \Phi_1 + m_{22}^2 \Phi_2^\dagger \Phi_2 \right] + \frac{1}{2} \left[\lambda_1 \left(\Phi_1^\dagger \Phi_1 \right)^2 + \lambda_2 \left(\Phi_2^\dagger \Phi_2 \right)^2 \right] \\ & + \lambda_3 \left(\Phi_1^\dagger \Phi_1 \right) \left(\Phi_2^\dagger \Phi_2 \right) + \lambda_4 \left(\Phi_1^\dagger \Phi_2 \right) \left(\Phi_2^\dagger \Phi_1 \right) + \frac{\lambda_5}{2} \left[\left(\Phi_1^\dagger \Phi_2 \right)^2 + \left(\Phi_2^\dagger \Phi_1 \right)^2 \right] \\ & - \frac{m_3^2}{2} \chi^* \chi + \lambda_{s1} (\chi^* \chi)^2 + \Lambda_1 (\Phi_1^\dagger \Phi_1) (\chi^* \chi) \\ & - \frac{m_4^2}{2} (\chi^{*2} + \chi^2) + \kappa_2 (\chi^3 + \chi^{*3}) + \kappa_3 [\chi (\chi^* \chi) + \chi^* (\chi^* \chi)]. \end{aligned} \quad (7)$$

Here, we have imposed a global $U(1)$ symmetry:

$$U(1) : \Phi_1 \rightarrow \Phi_1, \Phi_2 \rightarrow \Phi_2, \chi \rightarrow e^{i\alpha} \chi. \quad (8)$$

and kept only $U(1)$ -symmetric and $U(1)$ -soft-breaking terms of the most general IDMS potential [8].

Due to the imposed Z_2 -symmetry, the neutral scalar sector is divided into two separate sectors: the Z_2 -even Higgs sector, and the Z_2 -odd inert sector. The inert sector, H, A and H^\pm , is just like in the IDM, with H chosen to be the lightest inert particle, i.e. a DM candidate. Mass formulas for the inert particles from the IDM still hold, and they depend only on m_{22}^2 and $\lambda_{3,4,5}$. Note, that χ does not influence the inert sector in the cIDMS.

The Higgs sector is extended with respect to the IDM by addition of the singlet χ , which results in three Higgs particles h_1, h_2, h_3 . If $\Lambda_1, w, \sin \xi \neq 0$ then there is mixing between states of different CP properties. Relation between physical states $h_{1,2,3}$ and the base states with defined CP $\phi_{1,2,3}$ is given by:

$$\begin{pmatrix} h_1 \\ h_2 \\ h_3 \end{pmatrix} = R \begin{pmatrix} \phi_1 \\ \phi_2 \\ \phi_3 \end{pmatrix}, \quad (9)$$

where R is a 3×3 rotation matrix, that depends on three mixing angles (here and below $c_i = \cos \alpha_i$, $s_i = \sin \alpha_i$):

$$R = R_1 R_2 R_3 = \begin{pmatrix} c_1 c_2 & c_3 s_1 - c_1 s_2 s_3 & c_1 c_3 s_2 + s_1 s_3 \\ -c_2 s_1 & c_1 c_3 + s_1 s_2 s_3 & -c_3 s_1 s_2 + c_1 s_3 \\ -s_2 & -c_2 s_3 & c_2 c_3 \end{pmatrix}. \quad (10)$$

The rotation matrix and its inverse give us two important relations:

$$h_1 = c_1 c_2 \phi_1 + (c_3 s_1 - c_1 s_2 s_3) \phi_2 + (c_1 c_3 s_2 + s_1 s_3) \phi_3, \quad (11)$$

$$\phi_1 = c_1 c_2 h_1 - c_2 s_1 h_2 - s_2 h_3, \quad (12)$$

which describe the composition of the SM-like Higgs boson h_1 , in terms of real components ϕ_1 and ϕ_2 , which provide a CP-even part, as well as the ϕ_3 component – CP-odd one. Equivalently, one can look at it as the modification of the real component of the SM-like Higgs doublet Φ_1 from the cIDMS with respect to the SM and the IDM. Especially important is the first element both in R and R^{-1} equal to:

$$R_{11} = R_{11}^{-1} = c_1 c_2. \quad (13)$$

This matrix element gives the relative modification of the interaction of the Higgs boson (h_1) with respect to the IDM, and is important both in the LHC analysis, and in the DM studies.

3.1. Constraints

The parameter space of the cIDMS is constrained by current theoretical and experimental results. We follow the limits that we use for the IDM, described in the previous section, and we ascertain that the extended scalar sector is not violating any of those constraints. In our analysis we have checked the agreement with LEP results on invisible decays of W^\pm, Z and lower mass limit of the charged scalar; perturbativity conditions, which constrain mass splittings of inert particles in the heavy mass regime; EWPT limits, which test the influence of both inert scalars and additional Higgs particles. Furthermore, we shall demand that the lightest Higgs particle, h_1 is a SM-like Higgs with mass $M_{h_1} = 125$ GeV, and that it is in agreement with the latest LHC results. Finally, we will check that H is a good DM candidate, with proper relic density and within direct detection limits.

3.2. LHC Phenomenology

Latest LHC results provide further constraints on the parameters of the model. We consider the signal strengths $\mathcal{R}_{gg}, \mathcal{R}_{\gamma\gamma}, \mathcal{R}_{Z\gamma}, \mathcal{R}_{VV}$. According

to (12) the couplings of the lightest Higgs particle (h_1) with vector bosons and top quark get modified, as compared with the SM, only by a factor R_{11} (eq. (13)). The one-loop coupling of h_1 to photons receives contributions mainly from the W boson and top quark, as well as the charged scalar H^\pm from the inert sector. Thus, we can write the relevant h_1 decay widths as follows³:

$$\Gamma(h_1 \rightarrow XX) = R_{11}^2 \Gamma(\phi_{SM} \rightarrow XX), \quad XX = gg, VV^*,$$

$$\Gamma(h_1 \rightarrow \gamma\gamma) = R_{11}^2 |1 + \eta_{\gamma\gamma}|^2 \Gamma(\phi_{SM} \rightarrow \gamma\gamma), \quad \eta_{\gamma\gamma} = \frac{g_{h_1 H^+ H^-} v}{2R_{11} M_{H^\pm}^2} \left(\frac{A_{H^\pm}}{A_W^{SM} + A_t^{SM}} \right),$$

and analogous formula for $\Gamma(h_1 \rightarrow Z\gamma)$. Note, that the triple coupling $\lambda_{h_1 H^+ H^-}$ is given by $g_{h_1 H^+ H^-} = v\lambda_3 R_{11}$, meaning it is also modified with respect to the IDM by a factor of R_{11} . Finally, the signal strengths can be written as follows,

$$\mathcal{R}_{ZZ} = R_{11}^2 \zeta^{-1}, \quad \mathcal{R}_{\gamma\gamma} = R_{11}^2 |1 + \eta_{\gamma\gamma}|^2 \zeta^{-1}, \quad \mathcal{R}_{Z\gamma} = R_{11}^2 |1 + \eta_{Z\gamma}|^2 \zeta^{-1},$$

where ζ is defined as

$$\zeta \equiv 1 + \frac{\Gamma_{\text{inv}}}{R_{11}^2 \Gamma_{\text{tot}}^{SM}},$$

with Γ_{inv} corresponding to invisible decays of h_1 into inert particles (if $M_{H,A} < M_{h_1}/2$), and Γ_{tot}^{SM} being the total decay width of the SM Higgs boson. Notice that $\mathcal{R}_{ZZ} \leq 1$, while both $\mathcal{R}_{\gamma\gamma}$ and $\mathcal{R}_{Z\gamma}$ can exceed 1. If $\mathcal{R}_{\gamma\gamma} < 1$ then both $\mathcal{R}_{Z\gamma}$ and \mathcal{R}_{ZZ} are correlated with $\mathcal{R}_{\gamma\gamma}$, $\mathcal{R}_{\gamma\gamma} \sim \mathcal{R}_{Z\gamma}$ and $\mathcal{R}_{\gamma\gamma} \sim \mathcal{R}_{ZZ}$ (Fig. 2). There is a possibility of similar enhancement of both $\mathcal{R}_{\gamma\gamma}$ and $\mathcal{R}_{Z\gamma}$. This is in agreement with the IDM, where a correlation between enhancement in $\gamma\gamma$ and $Z\gamma$ channels exists [39].

For smaller values of M_{H^\pm} there is a possibility of enhancement of both $\mathcal{R}_{\gamma\gamma}$ (Fig. 2) and $\mathcal{R}_{Z\gamma}$. For heavier M_{H^\pm} the maximum values tend to the SM value, with a possible deviation up to 20 %. This is again a result similar to the one from the IDM, where significant enhancement, e.g. $\mathcal{R}_{\gamma\gamma} = 1.2$, was possible only if $M_{H^\pm} \lesssim 150$ GeV, and for heavier masses $\mathcal{R}_{\gamma\gamma} \rightarrow 1$ [39].

3.3. DM Phenomenology

The cIDMS can be treated as an extension of the IDM, and certain properties of DM sector are kept here. As there is no direct coupling between the inert doublet Φ_2 and the singlet χ , and the only interaction is through mixing of χ with Φ_1 , the inert particles' interaction with gauge bosons is like in the IDM, while the inert scalars-Higgs boson interaction changes. The IDM Higgs particle h corresponds in our case to ϕ_1 , so $h \rightarrow \phi_1$, where

³ See Appendix A in [8] and references therein for more details.

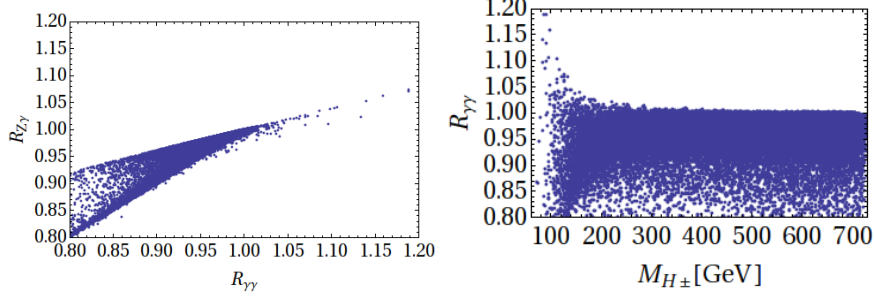


Fig. 2. Left: Correlation between $\mathcal{R}_{\gamma\gamma}$ and $\mathcal{R}_{Z\gamma}$. Right: Correlation between $\mathcal{R}_{\gamma\gamma}$ and M_{H^\pm} . Plots taken from [8].

ϕ_1 in terms of physical fields is given by (12). In our analysis we are focusing on the SM-like scenario, which corresponds to $c_1 c_2 \approx 1$. This would naively suggest that for all purposes we could keep $h \approx h_1$, and neglect the contribution from additional Higgs particles. However, our study shows that even if $c_1 c_2 \approx 1$ there are significant differences with respect to the IDM in relic density values coming from additional annihilation channels, interference and resonance effects due to the extended Higgs sector.

3.3.1. Benchmark Points

The analysis of DM properties was done for a couple of benchmarks⁴ chosen in agreement with constraints from LHC/LEP:

$$\mathbf{A1}: M_{h_1} = 124.83\text{GeV}, M_{h_2} = 194.46\text{GeV}, M_{h_3} = 239.99\text{GeV},$$

$$\mathbf{A4}: M_{h_1} = 125.36\text{GeV}, M_{h_2} = 149.89\text{GeV}, M_{h_3} = 473.95\text{GeV}.$$

The above values were chosen to illustrate different possible scenarios: in **A1** all Higgs particles are relatively light, but only h_1 is lighter than $2M_W$; for **A4** there are two Higgs particles that have mass below $2M_W$: h_1 (the SM-like Higgs) and h_2 . We treat $2M_W$ as the distinguishing value as two Higgs particles with $M_{h_i} < 2M_W$ influence the DM phenomenology by introducing another resonance region in the medium DM mass regime.

3.3.2. Low, Medium and Heavy Mass Regions

The cIDMS can provide a good DM candidate, with relic density in agreement with Planck results, in three regions of masses:

- Light DM mass: $53\text{ GeV} \lesssim M_H \lesssim M_{h_1}/2$ with $M_A, M_{H^\pm} \gtrsim M_H + 50\text{ GeV}$.

⁴ Additional benchmarks are discussed in [8].

Here, we observe no significant differences between benchmarks, because the main DM annihilation channel is the near-resonance $HH \rightarrow h_1 \rightarrow b\bar{b}$, thus making annihilation through heavier $h_{2,3}$ negligible. As in the IDM, the value of coupling that is in agreement with direct detection limits, LHC results and relic density measurements is very small, $\lambda_{345} \sim 0.002$ [8].

- Medium DM mass: $M_{h_1}/2 \lesssim M_H \lesssim M_W$ with $M_A, M_{H^\pm} \gtrsim M_H + 50$ GeV. Figure 3 shows the relation between parameter λ_{345} (which is closely related to the DM-Higgs coupling, $g_{HHh_1} = c_1 c_2 \lambda_{345}$, with $c_1 c_2 \approx 1$ for all SM-like scenarios) and DM mass M_H for benchmark A1 and A4. Benchmark A1, where both additional Higgs particles are heavier than $2M_W$, follows the well-known behaviour of the IDM. However, the presence of these additional states is non-negligible, as the annihilation of DM particles is enhanced and therefore the relic density for a given mass is lower with respect to DM candidate from the IDM [8].

A significant difference with respect to the IDM is visible if one of the extra Higgs bosons is lighter than $2M_W$, which is the case for benchmark A4. The annihilation rate is enhanced and dominated by the Higgs-type resonance exchange through h_2 (note the symmetric distribution around $\lambda_{345} = 0$), in contrast to the previously discussed cases [8].

- Heavy DM mass: $M_H \gtrsim 525$ GeV with $M_A = M_{H^\pm} = M_H + 1$ GeV. Again, we observe no significant differences between benchmarks, and this region reproduces DM phenomenology from the IDM. This is because the heavy DM candidate annihilates mostly through gauge (co)annihilation channels, therefore the extended scalar sector has minimal influence on the results.

3.3.3. Direct Detection Limits

The cIDMS, as other scalar DM models, can be strongly constrained by results of direct detection experiments. The current strongest limits come from LUX experiment [41]. As is the case with many other scalar DM models, the constraints are not strong enough for heavy DM candidate, as the sensitivity of direct detection experiments reduces significantly with increasing DM mass. The near resonance region $53 \text{ GeV} \lesssim M_H \lesssim 63 \text{ GeV}$ also escapes detection, due to very small value of Higgs-DM coupling⁵.

Fig. 3 presents the value of DM-nucleus scattering cross-section, $\sigma_{DM,N}$, for medium DM mass region, along with the latest LUX limit. Red regions denote benchmark A1, while blue regions correspond to benchmark A4. The difference between those two groups is clear. In case of benchmark A4, the coupling is usually much smaller than in case A1, therefore the resulting

⁵ Recall that the DM scattering off nuclei is mediated by the Higgs particles, h_1, h_2, h_3 , therefore the strength of this scattering will directly depend on the value of DM-Higgs couplings.

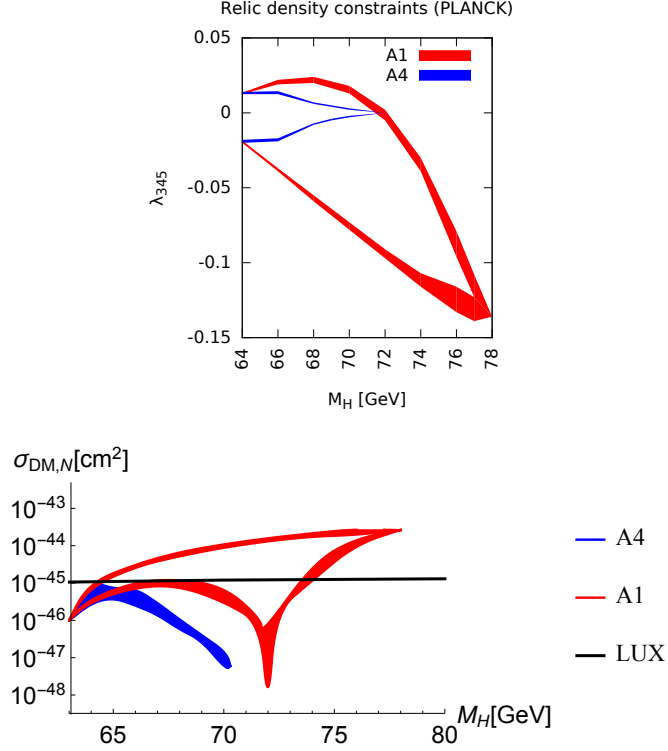


Fig. 3. Up: Relic density constraints on the mass of the DM candidate (M_H) and its coupling to SM Higgs boson. Red and blue regions corresponds to relic density in agreement with Planck measurements for benchmark A1 and A4, respectively. Down: DM-nucleus scattering cross-section for benchmarks A1 (red) and A4 (blue), with respect to LUX limits.

cross-section will be also smaller, falling well below the current experimental limits.

3.4. Comparison with the IDM

Both the IDM, and the cIDMS, can provide a good DM candidate, which is in agreement with the current experimental results. In both models, it is not possible to fulfil LHC constraints for the Higgs invisible decay branching ratio and relic density measurements at the same time if $M_H \lesssim 53$ GeV. Masses $53 \text{ GeV} \lesssim M_H \lesssim 63 \text{ GeV}$ correspond to the resonance region of enhanced annihilation with very small coupling λ_{345} . It is important to stress that, while DM phenomenology of the cIDMS does not depend on the chosen benchmark point (A1-A4), there is a difference when it comes to

the LHC observables. Values of $\mathcal{R}_{\gamma\gamma}$ for benchmark A4 are smaller than in all other cases – and smaller than the IDM – being always below 1.

For heavier DM mass, the extended scalar sector significantly changes the annihilation rate of DM particles. Our studies show that the annihilation cross-section is enhanced with respect to the IDM and therefore relic density in the cIDMS is usually lower than for the corresponding point in the IDM. Especially important is the possibility of having a second resonance region, that will mimic the low DM mass behaviour, if the mass of one of additional Higgs particles is smaller than $2M_W$. Corresponding DM-Higgs couplings, and thus the resulting $\sigma_{DM,N}$, constrained by results of direct detection experiments, is much smaller for A4 than for other benchmark points.

Heavy DM mass region resembles the IDM very closely. In the heavy mass region all inert particles are heavier than the particles from the SM sector and the impact on the Higgs phenomenology can be minimal. For example, this is the region where $\mathcal{R}_{\gamma\gamma}$ is the closest to the SM value.

The possibility of having CP violation is a significant modification of our model with respect to the IDM. It changes not only interaction in the Higgs sector, by allowing three states h_1 , h_2 and h_3 to have non-zero coupling to VV pairs, but also influences the DM sector, which itself – by construction – is CP conserving. CP violation in the Higgs sector changes the annihilation channels; for example, channels like $HH \rightarrow h_i \rightarrow Zh_j$ can appear and significantly change the relic density value if DM particle is heavy enough.

4. The SM+CS: The SM plus a complex singlet

As stated before, the CP violation in the SM is insufficient to explain the baryon asymmetry in the Universe and therefore an additional source of CP-violation is needed. The simplest possibility is through the extension of SM with a complex singlet [42, 43]. We consider such a scenario according to which the SM-like Higgs particle comes mostly from the SM-like SU(2) doublet, with a small modification coming from the singlet. Note, that this is a part of the IDMS responsible for the CP violation.

The scalar potential of the model, with assumption on U(1) symmetry as in cIDMS (8), can be written as:

$$V = -\frac{1}{2}m_{11}^2\Phi_1^\dagger\Phi_1 + \frac{1}{2}\lambda_1\left(\Phi_1^\dagger\Phi_1\right)^2 - \frac{m_s^2}{2}\chi^*\chi + \lambda_{s1}(\chi^*\chi)^2 + \Lambda_1(\Phi_1^\dagger\Phi_1)(\chi^*\chi) - \frac{m_4^2}{2}(\chi^{*2} + \chi^2) + \kappa_2(\chi^3 + \chi^{*3}) + \kappa_3[\chi(\chi^*\chi) + \chi^*(\chi^*\chi)]. \quad (14)$$

Φ_1 and χ fields acquire vacuum expectation values v and $we^{i\xi}$, respectively, where $v, w, \xi \in \mathbf{R}$. We shall use the following field decomposition around

the vacuum state:

$$\Phi_1 = \left(\begin{array}{c} \phi_1^+ \\ \frac{1}{\sqrt{2}}(v + \phi_1 + i\phi_4) \end{array} \right), \quad \chi = \frac{1}{\sqrt{2}}(we^{i\xi} + \phi_2 + i\phi_3). \quad (15)$$

We assume that all parameters of V (14) are real. There are three quadratic parameters, six dimensionless quartic parameters and five dimensionful parameters κ_i , $i = 1, 2, 3, 4, 5$. The linear term κ_1 can be removed by a translation of the singlet field, and therefore neglected.

In order to have a stable minimum, the parameters of the potential have to satisfy the positivity conditions. Particularly, the potential should be bounded from below, i.e. should not go to negative infinity for large field values. As this behavior is dominated by the quartic terms, the cubic terms will not play a role here. Thus, the following conditions will apply to a variety of models that will differ only by their cubic interactions. The positivity conditions read:

$$\lambda_1, \lambda_{s1} > 0, \quad \bar{\lambda}_{1S} = \Lambda_1 + \sqrt{2\lambda_1\lambda_{s1}} > 0. \quad (16)$$

4.1. Extremum conditions

It is useful to decompose complex fields into two real fields S_1, S_2 with respective VEVs w_1, w_2 :

$$\chi = (S_1 + iS_2)/\sqrt{2}, \quad \chi^* = (S_1 - iS_2)/\sqrt{2}, \\ \langle \chi \rangle = we^{i\xi} = \underbrace{w \cos \xi}_{w_1} + i \underbrace{w \sin \xi}_{w_2}, \quad w_1^2 + w_2^2 = w^2. \quad (17)$$

For potential (14), we got the following extremum conditions:

$$-m_{11}^2 + \lambda v^2 + \Lambda_1 w^2 = 0, \quad (18)$$

$$w_1(-m_s^2 - 2m_4^2 + v^2\Lambda_1 + 2w^2\lambda_{s1}) + 3\sqrt{2}(w_1^2 - w_2^2)\kappa_2 \\ + \sqrt{2}(3w_1^2 + w_2^2)\kappa_3 = 0, \quad (19)$$

$$w_2(-m_s^2 + 2m_4^2 + v^2\Lambda_1 + 2w^2\lambda_{s1} + 2\sqrt{2}w_1(-3\kappa_2 + \kappa_3)) = 0. \quad (20)$$

We will keep w_1 and w_2 non-zero, noticing that only when $w_2 \neq 0$, there is a non-zero phase of χ . Performing the subtraction of equation (19) from equation (20) we obtain an important relation between parameters:

$$-4m_4^2 \cos \xi + 3R_2(1 + 2\cos 2\xi) + R_3 = 0, \quad (21)$$

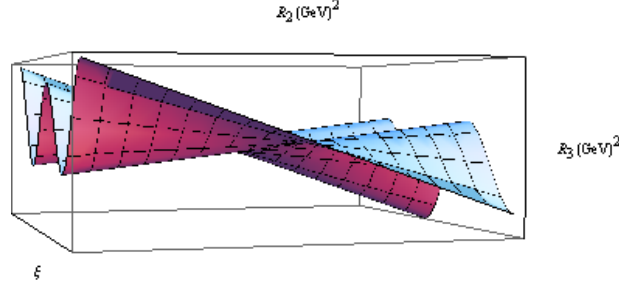


Fig. 4. (R_2, R_3, ξ) for $m_4^2 = 500 \text{ GeV}^2$.

where $R_2 = \sqrt{2}w^2\kappa_2$ and $R_3 = \sqrt{2}w^2\kappa_3$. This relation describes the region of parameters in which CP violation may occur. The CP violation in the SM+CS model, due to non-zero phase of the complex singlet, may be realized in wide regions determined by quadratic and cubic parameters from V . Fig. 4 and Fig. 5 show regions of parameter space where this relation holds. Fig. 4 shows the correlation between R_2 , R_3 and ξ for $m_4^2 = 500 \text{ GeV}^2$, while Fig. 5 presents the $4m_4^2$ against the R_3 for $R_2=0$.

One can conclude that for the existence of a viable CP violation in the model it is necessary to have at least two non-vanishing variables among R_2 , R_3 , m_4^2 .

5. Conclusions

The Inert Doublet Model is simple, yet very powerful, extension of the SM scalar sector. It can provide a good DM candidate, and at the same time accommodate the SM-like Higgs signal. The IDM is in agreement with all current experimental data. However, the IDM is missing one crucial ingredient to explain the baryon asymmetry of the Universe, i.e. the additional source of CP violation. Further extensions of the IDM, e.g. by a complex singlet, can solve this problem, by introducing explicit or spontaneous CP

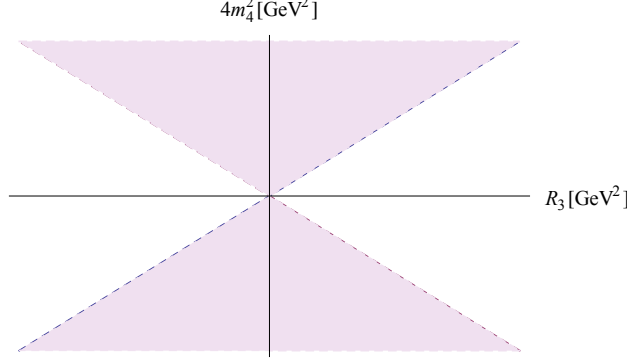


Fig. 5. (R_3, m_4^2) for $R_2 = 0$, $\cos \xi \in (-1, 1)$.

violation in the scalar sector. Furthermore, the extended scalar sector can influence the DM phenomenology, including not only changes in DM annihilation scenarios, but also changing prospects of DM detection, either by dedicated DM direct detection experiments, or by the LHC.

6. Acknowledgments

MK and ND would like to thank organizers of this and all previous Schools one of us attended. Presented results were obtained in fruitful collaborations with B. Świeżewska, P. Swaczyna, J. L. Diaz-Cruz and C. Bonilla.

The work was partially supported by the grant NCN OPUS 2012/05/B/ST2/03306 (2012-2016).

REFERENCES

- [1] N. G. Deshpande and E. Ma, *Phys.Rev.* **D18** (1978) 2574.
- [2] E. Ma, *Phys.Rev.* **D73** (2006) 077301,
- [3] R. Barbieri, L. J. Hall and V. S. Rychkov, *Phys. Rev.* **D74** (2006) 015007.
- [4] M. Krawczyk, D. Sokolowska, P. Swaczyna and B. Swiezewska, *JHEP* **1309** (2013) 055.
- [5] A. Ilnicka, M. Krawczyk and T. Robens, arXiv:1508.01671 [hep-ph], A. Ilnicka, M. Krawczyk and T. Robens, PoS(EPS-HEP2015)143 [arXiv:1510.04159 [hep-ph]].
- [6] I. F. Ginzburg, K. A. Kanishev, M. Krawczyk and D. Sokolowska, *Phys. Rev. D* **82** (2010) 123533 [arXiv:1009.4593 [hep-ph]].
- [7] G. Gil, P. Chankowski and M. Krawczyk, *Phys. Lett. B* **717**, 396 (2012) [arXiv:1207.0084 [hep-ph]].

- [8] C. Bonilla, D. Sokolowska, N. Darvishi, J. L. Diaz-Cruz and M. Krawczyk, arXiv:1412.8730 [hep-ph].
- [9] M. Krawczyk and D. Sokolowska, “Constraining the Dark 2HDM,” 2009, 0911.2457.
- [10] D. Sokolowska, *Acta Phys.Polon.* **B42** (2011) 2237.
- [11] D. Sokolowska, arXiv:1104.3326 [hep-ph].
- [12] D. Sokolowska, “Dark Matter Data and Constraints on Quartic Couplings in IDM,” 2011, 1107.1991.
- [13] L. Lopez Honorez, E. Nezri, J. F. Oliver and M. H. G. Tytgat, *JCAP* **0702** (2007) 028.
- [14] M. H. Tytgat, “The Inert Doublet Model: A New archetype of WIMP dark matter?,” *J.Phys.Conf.Ser.*, vol. 120, p. 042026, 2008, 0712.4206.
- [15] Q.-H. Cao, E. Ma and G. Rajasekaran, *Phys.Rev.* **D76** (2007) 095011.
- [16] M. Gustafsson, E. Lundstrom, L. Bergstrom, and J. Edsjo, “Significant gamma lines from inert higgs dark matter,” 2007, astro-ph/0703512.
- [17] P. Agrawal, E. M. Dolle, and C. A. Krenke, “Signals of Inert Doublet Dark Matter in Neutrino Telescopes,” *Phys.Rev.*, vol. D79, p. 015015, 2009, 0811.1798.
- [18] E. Lundstrom, M. Gustafsson and J. Edsjo, *Phys. Rev. D* **79** (2009) 035013 [arXiv:0810.3924 [hep-ph]].
- [19] E. M. Dolle and S. Su, *Phys.Rev.* **D80** (2009) 055012.
- [20] E. Dolle, X. Miao, S. Su, and B. Thomas, “Dilepton Signals in the Inert Doublet Model,” *Phys.Rev.*, vol. D81, p. 035003, 2010, 0909.3094.
- [21] C. Arina, F.-S. Ling, and M. H. Tytgat, “IDM and iDM or The Inert Doublet Model and Inelastic Dark Matter,” *JCAP*, vol. 0910, p. 018, 2009, 0907.0430.
- [22] E. Lundstrom, M. Gustafsson, and J. Edsjo, “The Inert Doublet Model and LEP II Limits,” *Phys.Rev.*, vol. D79, p. 035013, 2009, 0810.3924.
- [23] M. Gustafsson, “The Inert Doublet Model and Its Phenomenology,” *PoS*, vol. CHARGED2010, p. 030, 2010, 1106.1719.
- [24] A. Heister *et al.* [ALEPH Collaboration], *Phys. Lett. B* **543** (2002) 1 [hep-ex/0207054].
- [25] L. Lopez Honorez and C. E. Yaguna, *JHEP* **1009** (2010) 046.
- [26] L. Lopez Honorez and C. E. Yaguna, *JCAP* **1101** (2011) 002.
- [27] S. Kanemura, T. Kubota, and E. Takasugi, “Lee-Quigg-Thacker bounds for Higgs boson masses in a two doublet model,” *Phys.Lett.*, vol. B313, pp. 155–160, 1993, hep-ph/9303263.
- [28] A. G. Akeroyd, A. Arhrib, and E.-M. Naimi, “Note on tree level unitarity in the general two Higgs doublet model,” *Phys.Lett.*, vol. B490, pp. 119–124, 2000, hep-ph/0006035.
- [29] B. Swiezewska, “Yukawa independent constraints for 2HDMs with a 125 GeV Higgs boson,” 2012, 1209.5725.

- [30] M. E. Peskin and T. Takeuchi, Phys. Rev. Lett. **65** (1990) 964. doi:10.1103/PhysRevLett.65.964; M. E. Peskin and T. Takeuchi, Phys. Rev. D **46** (1992) 381. doi:10.1103/PhysRevD.46.381
- [31] K. Nakamura *et al.*, “Review of particle physics,” *J.Phys.G*, vol. G37, p. 075021, 2010.
- [32] Dorota Sokołowska, PhD Thesis 2013 ”Evolution of the Universe in Two Higgs Doublet Model”
- [33] G. Aad *et al.* [ATLAS and CMS Collaborations], Phys. Rev. Lett. **114** (2015) 191803 [arXiv:1503.07589 [hep-ex]].
- [34] The CMS Collaboration, *Phys. Lett. B* **736**, 64 (2014),
- [35] ATLAS-CONF-2015-044, CMS-PAS-HIG-15-002
- [36] The ATLAS Collaboration, ATLAS-CONF-2014-010 (2014), G. Aad *et al.* [ATLAS Collaboration], arXiv:1509.00672 [hep-ex]; CMS Collaboration [CMS Collaboration], CMS-PAS-HIG-15-012.
- [37] P. Posch, “Enhancement of $h \rightarrow \gamma\gamma$ in the Two Higgs Doublet Model Type I,” *Phys.Lett.*, vol. B696, pp. 447–453, 2011, 1001.1759.
- [38] A. Arhrib, R. Benbrik, and N. Gaur, “ $H \rightarrow \gamma\gamma$ in Inert Higgs Doublet Model,” *Phys.Rev.*, vol. D85, p. 095021, 2012, 1201.2644.
- [39] B. Swiezewska and M. Krawczyk, “Diphoton rate in the Inert Doublet Model with a 125 GeV Higgs boson,” Phys. Rev. D **88** (2013) 035019 [arXiv:1212.4100 [hep-ph]].
- [40] Planck Collaboration, arXiv:1303.5076 [hep-ex].
- [41] D. Akerib *et al.*, arXiv:1310.8214 [hep-ex].
- [42] G. C. Branco, P. A. Parada and M. N. Rebelo, hep-ph/0307119.
- [43] L. Bento, G. C. Branco and P. A. Parada, Phys. Lett. B **267** (1991) 95. doi:10.1016/0370-2693(91)90530-4